DALTON
FULL PAPER

Hydrogen bonds in crystals of HO-(N∩N′)M(CO)$_3$L complexes: chains, dimers and an unexpected hexamer † ‡

Katja Heinze * and Volker Jacob

Anorganisch-Chemisches Institut der Universität Heidelberg, Im Neuenheimer Feld 270, 69120 Heidelberg, Germany. E-mail: katja.heinze@urz.uni-heidelberg.de

Received 14th February 2002, Accepted 27th March 2002
First published as an Advance Article on the web 2nd May 2002

Complexes of the type [HO-(N∩N′)]M(CO)$_3$L (M = Cr, Mo, W; L = CO, CN*t*Bu) have been prepared and characterised and their crystal structures have been determined by X-ray crystallography. The aggregation of the complexes in the solid state follows general patterns due to the formation of multiple hydrogen bonds giving infinite chains, dimers and a cyclic hexamer. The hydrogen bonding in the solid state is also detected and analysed by IR spectroscopy and corroborated by DFT calculations.

Introduction

Within our research on performing organometallic chemistry on solid supports [1,2] we prepared and characterised a number of carbonyl complexes of group VI metals with a chelating Schiff base ligand 4-[(pyridine-2-ylmethylene)amino]phenol HO-(N∩N′) containing a pendant phenol group. The inspection of the crystal structures of the molybdenum carbonyl complexes [HO-(N∩N′)]Mo(CO)$_3$L (L = THF, CO, PPh$_3$, CN*t*Bu, CNCy) revealed several intermolecular interactions between individual molecules.[3] Hydrogen bonds between coordinated carbonyl groups as hydrogen acceptors and the phenolic hydroxo groups as well as CH groups of the Schiff base ligands as hydrogen donors appear as the most prominent structural motif. Although hydrogen bonding [4,5] has been of great importance in supramolecular chemistry and in the field of crystal engineering [6] general rules for the prediction and explanation of the aggregation of molecules in the solid state are still lacking – especially for organometallic complexes. Consequently our research is extended to the chromium and tungsten analogues with the aim of generalising the observed aggregation patterns to a broader class of complexes. In addition IR spectroscopy combined with theoretical calculations is used to probe the intermolecular hydrogen bonding interactions.

Results and discussion

The chromium and tungsten carbonyl complexes **1a/1c** and **2a/2c** (Scheme 1) were prepared by procedures similar to those of the corresponding molybdenum complexes **1b** and **2b** (see Experimental section).[3] All new complexes have been characterised in solution by NMR, IR and UV/Vis spectroscopy confirming the assigned molecular structures.

The IR spectra in solution (Fig. S1 and S2, see ESI ‡) are consistent with a disturbed local C_{2v} symmetry of the *cis*-tetracarbonyl complexes **1** and with disturbed local C_{3v} symmetry of the *fac*-tricarbonyl complexes **2**. The latter complexes additionally show a medium strong absorption for the CN stretching vibration. The electronic spectra of **1a–c** and **2a–c** show metal-to-ligand charge transfer (MLCT) absorption bands in the ranges 537–571 nm (**1a–c**) and 618–665 nm (**2a–c**). For the stronger π-acceptor ligand CO (complexes **1**) the MLCT bands occur at higher energies as expected.[2,7,8,9,10] The geometry of the complexes in the solid state has been determined by single crystal X-ray analysis. Selected bond lengths and angles are shown in Tables 1 and 2.

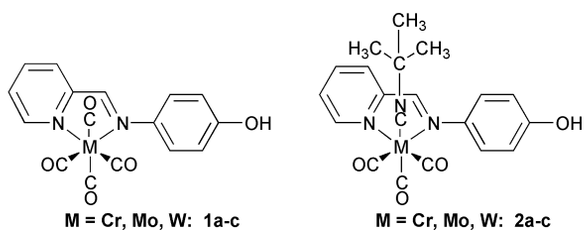

Scheme 1 Complexes **1a–c** and **2a–c**.

The metal ligand bond lengths M–N and M–C increase from Cr (**1a/2a**) to Mo (**1b/2b**) but remain almost constant for the Mo and W complexes (**1b/2b**; **1c/2c**) as a consequence of the similar atomic radii of molybdenum and tungsten. Other local geometric features of the individual complexes appear to be independent of the central metal, except for the different torsion angles C7–N1–C1–C2 of the phenol ring with respect to the imine plane of the ligand in complexes **1**: the absolute torsion angle is smaller for **1a** by 10° (Table 2). This difference may be caused by the different size of the atomic radius of Cr together with the different arrangement of the complexes in the solid state (*vide infra*).

1a crystallises in the trigonal space group $R\bar{3}$ without inclusion of solvent molecules. The structure consists of coaxial stacks of hydrogen bonded cyclic hexamers parallel to the short *c*-axis. Each hexamer has $\bar{3}$ symmetry and is held together – at first sight – only by O–H ··· O hydrogen bonds forming a motif of graph set $R^6_6(12)$ [11] (Table 3, Scheme 2, Fig. 1 top).

Only few examples of hydrogen bonded cyclic hexamers (Fig. 1, bottom) can be found in the literature. In the crystal structure of bis(pentafluorphenyl)methanol [12] the individual units are also related by $\bar{3}$ symmetry as are the six water molecules in an oxovanadate inclusion compound [13] whereas the iron dithiolate complex D,L-[Fe$_2${SCH$_2$CH–CH$_2$OH)S}(CO)$_6$] [14] and the six water molecules in the inclusion compound 2,4-dimethyl-5-aminobenzo[*b*]-1,8-napththyridine [15] form hexamers

† Dedicated to Prof. Dr. G. Huttner on the occasion of his 65th birthday.

‡ Electronic supplementary information (ESI) available: solution IR spectra of **1a–1c** and **2a–2c**; selected structures; DFT optimised coordinates, selected harmonic frequencies, IR intensities and normal coordinates, selected bond lengths and bond angles for HOLMo(CO)$_3$CNCH$_3$ and HOLMo(CO)$_3$CNCH$_3$·H$_2$O. See http://www.rsc.org/suppdata/dt/b2/b201647h/

DOI: 10.1039/b201647h

Table 1 Selected bond lengths (Å) of **1a**, **1b**, **1c**, **2a**, **2b** and **2c**

	1a M = Cr E = O16	**1b** M = Mo E = O16	**1c** M = W E = O16	**2a** M = Cr E = N3	**2b** M = Mo E = N3	**2c** M =W E = N3
M–N1	2.118(2)	2.265(5)	2.243(6)	2.103(1)	2.247(2)	2.228(9)
M–N2	2.110(2)	2.226(6)	2.226(7)	2.121(2)	2.254(2)	2.25(1)
M–C13	1.847(3)	1.957(7)	1.956(8)	1.846(2)	1.958(3)	1.96(1)
M–C14	1.885(3)	2.024(8)	2.035(8)	1.869(2)	1.997(3)	1.99(1)
M–C15	1.833(3)	1.971(7)	1.974(9)	1.821(2)	1.931(3)	1.94(1)
M–C16	1.919(3)	2.072(8)	2.070(9)	2.023(2)	2.166(3)	2.17(1)
C13–O13	1.162(3)	1.161(8)	1.172(9)	1.163(2)	1.159(3)	1.18(1)
C14–O14	1.160(3)	1.148(8)	1.13(1)	1.153(2)	1.148(3)	1.16(1)
C15–O15	1.170(3)	1.163(8)	1.16(1)	1.176(2)	1.180(3)	1.19(1)
C16–E	1.147(3)	1.136(8)	1.12(1)	1.159(2)	1.159(3)	1.15(1)
N1–C7	1.292(3)	1.291(8)	1.27(1)	1.289(2)	1.290(3)	1.29(1)
N2–C8	1.363(3)	1.361(8)	1.36(1)	1.362(2)	1.362(3)	1.35(1)
C7–C8	1.449(4)	1.456(9)	1.46(1)	1.447(2)	1.443(4)	1.44(2)
N1–C1	1.440(3)	1.440(8)	1.45(1)	1.430(2)	1.434(3)	1.41(1)
O1–C4	1.380(3)	1.377(8)	1.38(1)	1.366(2)	1.369(3)	1.36(1)

Table 2 Selected bond angles (°) of **1a**, **1b**, **1c**, **2a**, **2b** and **2c**

	1a M = Cr	**1b** M = Mo	**1c** M = W	**2a** M = Cr	**2b** M = Mo	**2c** M = W
N1–M–N2	76.16(8)	72.9(2)	72.9(2)	75.68(6)	72.03(8)	72.1(3)
N1–M–C13	172.8(1)	167.4(2)	167.7(3)	170.37(7)	168.20(9)	167.5(4)
N1–M–C14	94.9(1)	95.3(2)	95.7(3)	92.95(7)	94.27(9)	93.7(4)
N1–M–C15	97.0(1)	101.3(2)	100.9(3)	101.06(7)	103.88(9)	103.1(4)
N1–M–C16	95.5(1)	90.7(2)	90.6(3)	84.34(7)	82.82(9)	83.1(4)
N2–M–C13	97.1(1)	94.6(2)	94.9(3)	94.77(7)	96.25(9)	95.5(4)
N2–M–C14	98.0(1)	93.2(2)	93.3(3)	88.49(7)	88.22(9)	88.3(3)
N2–M–C15	172.4(1)	173.2(2)	173.7(3)	175.26(7)	174.25(9)	173.8(4)
N2–M–C16	90.2(1)	91.7(2)	92.4(3)	90.09(6)	89.39(8)	88.9(4)
C13–M–C14	83.6(1)	83.6(3)	83.6(3)	87.94(8)	86.6(1)	87.4(5)
C13–M–C15	89.9(1)	91.2(3)	91.4(3)	88.54(8)	87.9(1)	89.3(5)
C13–M–C16	86.8(1)	91.2(3)	91.1(3)	94.61(8)	95.9(1)	95.3(5)
C14–M–C15	85.7(1)	85.6(3)	86.2(4)	88.23(8)	88.1(1)	88.2(5)
C14–M–C16	168.0(1)	173.2(3)	172.6(3)	177.18(8)	176.7(1)	176.3(5)
C15–M–C16	87.2(1)	90.1(3)	88.8(3)	93.03(8)	94.1(1)	94.4(5)
C7–N1–C1–C2	−130.6(3)	142.3(7)	141.2(8)	−134.7(2)	−138.6(2)	−138(1)
C7–C8–N2–C12	−177.0(2)	178.6(6)	178.6(7)	178.6(2)	178.8(2)	180(1)
C1–C6 ··· C1A–C6A[a]	—	3.6 Å/1°	3.6 Å/1°	—	—	—

[a] Distance between ring centres/angle between ring planes.

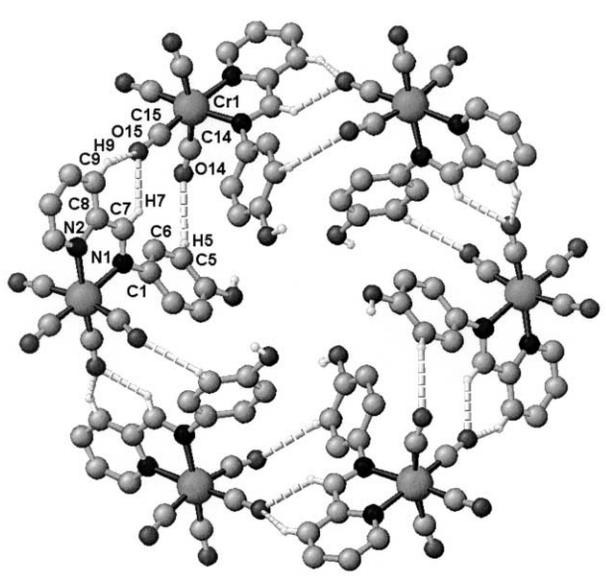

Fig. 1 View of the hexameric structure of **1a**; (top) $R^6_6(12)$ motif, (bottom) $R^6_6(36)$, $R^6_6(42)$ and $R^6_6(48)$ motifs.

with $\bar{1}$ symmetry. Common to all cyclic hexamers $(ROH)_6$ of graph set $R^6_6(12)$ is the chair conformation of the six oxygen atoms which is also found in hexagonal and cubic ice[16] and in the unstable cyclic water hexamer.[17–19] The chair conformation found in **1a** is among the most twisted ones with torsion angles O ··· O ··· O ··· O of ±60.5° and a displacement of the oxygen atoms from the mean plane of ±0.45 Å (Table 4). The O ··· O distance within the hexameric ring of **1a** is one of the shortest found experimentally[12–15] and calculated for the cyclic water hexamer[18,19] so far (Table 4).

In addition to the O–H ··· O hydrogen bonds, C–H ··· O hydrogen bonds[4] between hexamers within the stacks are observed (Table 3, Fig. 1 bottom). The latter form motifs of graph sets[11] $R^6_6(36)$, $R^6_6(42)$ and $R^6_6(48)$ with the *cis*-oriented carbonyl groups C14/O14 and C15/O15 as hydrogen acceptors and C5, C7 and C9 as hydrogen donors (AA ··· DDD type[20]). As these motifs span the stacked hexamers of the $R^6_6(12)$ motif with a Cr ··· Cr distance of 8.72 Å the stacks become further internally connected. Fig. 2 (middle) shows the full hydrogen bonding network in the crystal structure of **1a** as a combination of the $R^6_6(36)$, $R^6_6(42)$ and $R^6_6(48)$ motifs (Fig. 2, left) and the $R^6_6(12)$ motif (Fig. 2, right). In the centre of the stacks a small channel framed by oxygen atoms with a diameter of approximately 5 Å (O ··· O distance; void space diameter approximately 3.6 Å) is formed which appears to be too small to host *e.g.* solvent molecules.

The molybdenum and tungsten tetracarbonyl complexes **1b** and **1c** crystallise in the monoclinic space group $P2_1/c$ without solvent molecules. Between the individual molecules CH ··· O hydrogen bonds C7–H7 ··· O13, C9–H9 ··· O13 and C5–

Table 3 Main geometrical parameters for H ⋯ O contacts in the crystal structures of complexes **1** and **2** (in Å and °)

	D	A	D–H	H ⋯ A	D–H–A	D ⋯ A	Motif	Atoms
1a	C5–H5	O14	0.93	2.66	143.2	3.45	$R^6_6(48)$	O14–C14–Cr1–N1–C1–C6–C5–H5
	C7–H7	O15	0.93	2.41	142.2	3.19	$R^6_6(36)$	O15–C15–Cr1–N1–C7–H7
	C9–H9	O15	0.93	2.91	132.7	3.60	$R^6_6(42)$	O15–C15–Cr1–N2–C8–C9–H9
	O1–H1	O1	0.82	2.00	136.3	2.66	$R^6_6(12)$	O1–H1
1b	C7–H7	O1	1.00	2.61	128.7	3.33	C(8)	O1–C4–C3–C2–C1–N1–C7–H7
	C7–H7	O13	1.00	2.52	148.2	3.41	C(6)	O13–C13–Mo1–N1–C7–H7
	C9–H9	O13	0.93	2.50	149.8	3.34	C(7)	O13–C13–Mo1–N2–C8–C9–H9
	C2–H2	O15	0.93	2.68	146.6	3.50	C(7)	O15–C15–Mo1–N1–C1–C2–H2
	C5–H5	O15	0.93	2.79	121.6	3.37	C(8)	O15–C15–Mo1–N1–C1–C6–C5–H5
	C5–H5	O16	0.93	2.79	131.6	3.48	C(8)	O16–C16–Mo1–N1–C1–C6–C5–H5
	C1–6	C1–6	—	—	1	3.60		[b]
1c	C7–H7	O1	0.93	2.65	130.0	3.33	C(8)	O1–C4–C3–C2–C1–N1–C7–H7
	C7–H7	O13	0.93	2.60	143.5	3.40	C(6)	O13–C13–W1–N1–C7–H7
	C9–H9	O13	0.93	2.46	150.1	3.30	C(7)	O13–C13–W1–N2–C8–C9–H9
	C2–H2	O15	0.93	2.63	147.4	3.45	C(7)	O15–C15–W1–N1–C1–C2–H2
	C5–H5	O15	0.93	2.78	121.1	3.36	C(8)	O15–C15–W1–N1–C1–C6–C5–H5
	C5–H5	O16	0.93	2.77	130.6	3.45	C(8)	O16–C16–W1–N1–C1–C6–C5–H5
	C1–6	C1–6	—	—	1	3.60		[b]
2a	C12–H12	O1	0.98	2.54	121.4	3.16	C(10)	O1–C4–C3–C2–C1–N1–Cr1–N2–C12–H12
	C11–H11	O13	0.90	2.60	132.7	3.28	C(7)	O13–C13–Cr1–N2–C12–C11–H11
	C5–H5	O14	0.93	2.83	122.7	3.42	C(8)	O14–C14–Cr1–N1–C1–C6–C5–H5
	C3–H3	O15	0.93	2.83	131.8	3.52	$R^2_2(16)$	O15–C15–Cr1–N1–C1–C2–C3–H3
	O1–H1	O15	0.75	2.08	177.7	2.83	$R^2_2(20)$	O15–C15–Cr1–N1–C1–C2–C3–C4–O1–H1
2b	C12–H12	O1	0.94	2.58	123.9	3.20	C(10)	O1–C4–C3–C2–C1–N1–Mo1–N2–C12–H12
	C11–H11	O13	0.90	2.53	133.7	3.21	C(7)	O13–C13–Mo1–N2–C12–C11–H11
	C5–H5	O14	0.99	2.72	120.4	3.33	C(8)	O14–C14–Mo1–N1–C1–C6–C5–H5
	C3–H3	O15	0.88	2.76	132.3	3.43	$R^2_2(16)$	O15–C15–Mo1–N1–C1–C2–C3–H3
	O1–H1	O15	0.84	1.98	178.0	2.81	$R^2_2(20)$	O15–C15–Mo1–N1–C1–C2–C3–C4–O1–H1
2c	C12–H12	O1	0.93	2.57	123.1	3.18	C(10)	O1–C4–C3–C2–C1–N1–W1–N2–C12–H12
	C11–H11	O13	0.93	2.48	131.8	3.18	C(7)	O13–C13–W1–N2–C12–C11–H11
	C5–H5	O14	0.93	2.74	120.4	3.31	C(8)	O14–C14–W1–N1–C1–C6–C5–H5
	C3–H3	O15	0.93	2.77	128.8	3.43	$R^2_2(16)$	O15–C15–W1–N1–C1–C2–C3–H3
	O1–H1	O15	0.58	2.24	162.6	2.80	$R^2_2(20)$	O15–C15–W1–N1–C1–C2–C3–C4–O1–H1

[a] The C–H distances are directly extracted from the crystal structure determinations and are not normalised. All D ⋯ A distances <3.6 Å and D–H ⋯ A angles >120° are reported. The full report of all contacts is for completeness only, with the aim of extracting common features. Not all contacts are necessarily considered attractive in nature, which might be especially true for the CH ⋯ O contacts. [b] π–π interaction.

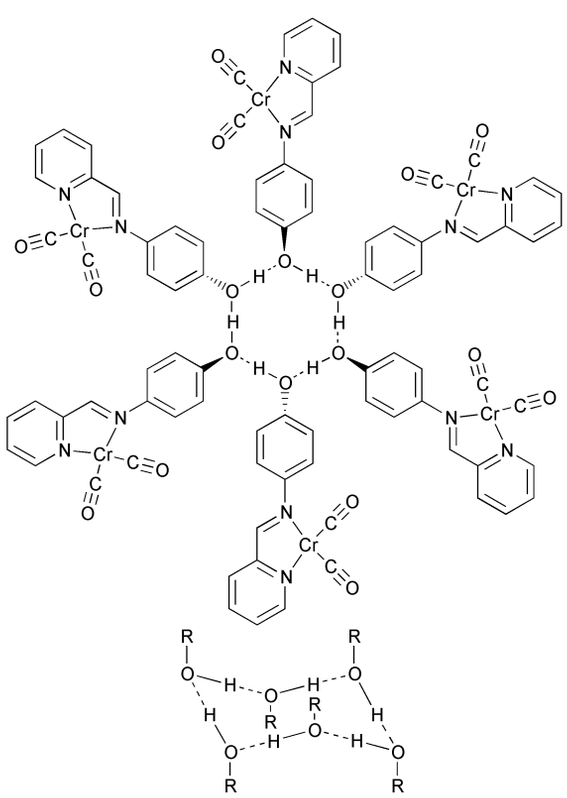

Scheme 2 Hexameric **1a** (top) and cyclic water–alcohol hexamer (bottom). Axial carbonyl ligands are omitted.

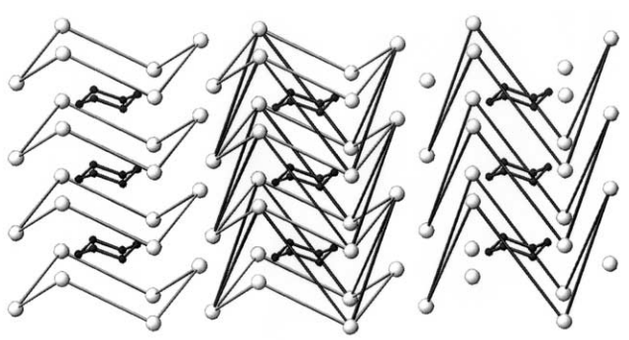

Fig. 2 Sketch of the hydrogen bonding network of **1a**. Cr atoms light-grey, O atoms dark-grey.

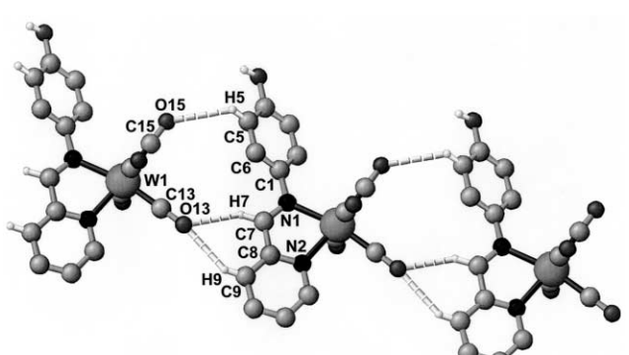

Fig. 3 Packing of **1c** (and **1b**) along the *a*-axis.

Table 4 Geometrical parameters of cyclic ROH hexamers

	O ··· O/Å	O–H ··· O/°	O ··· O ··· O/°	O ··· O ··· O ··· O/°	Mean plane displacement/Å
1a	2.66	136	109.3	±60.5	±0.45
$(C_6F_5)_2CHOH$ [12]	2.70	158	118.2	±26.1	±0.18
Oxovanadate H_2O inclusion [13]	2.77	177	100.1	±86.3	±0.64
D,L-[Fe_2{SCH_2CH–CH_2OH)S}-$(CO)_6$] [14]	2.67, 2.66, 2.67	168, 159, 171	99.5, 128.9, 113.5	±39.9, ±49.1, ±54.4	±0.31, ±0.28, ±0.39
2,4-Dimethyl-5-aminobenzo[*b*]-1,8-napththyridine H_2O inclusion [15]	2.79, 2.71, 2.83	171, 168, 145	140.2, 96.0, 113.2	±41.9, ±27.7, ±46.2	±0.23, ±0.22, ±0.29
H_2O (HF) [16]	2.85	177.5	117.4±31.5	±0.23	
H_2O (DFT) [17]	2.71	179.1	119.0	±19.6	±0.14

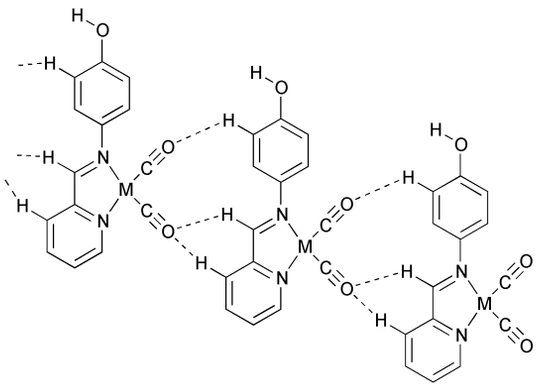

Scheme 3 Aggregation of **1b** and **1c** in the solid state with the C(6), C(7) and C(8) motifs. M = Mo, W. Axial carbonyl ligands are omitted.

H5 ··· O15 form chains of graph set C(6), C(7) and C(8), respectively (Table 3, Fig. 3, Scheme 3). These hydrogen bonds connect molecules translated along the crystallographic *a*-axis with repeat lengths of 9.05 Å (**1b**) and 9.00 Å (**1c**) forming a triple hydrogen bond of AA ··· DDD type. This triple hydrogen bond gives a similar connectivity as found for **1a** with the same hydrogen atoms of the Schiff base ligand (H5, H7, H9) involved and the same number of atoms present in each graph set.[21] The triple hydrogen bond motif of **1b/1c** differs from that of **1a** solely in the *cis*-dicarbonyl unit involved: in complexes **1b/1c** the equatorial CO groups (C13–O13 and C15–O15) act as acceptors for hydrogen bonding while complex **1a** employs one equatorial (C15–O15) and one axial (C14–O14) carbonyl group. This different attachment might also induce the different values of the torsion angles C7–N1–C1–C2 in **1a** and **1b/1c** (*vide supra*) as noted above (Table 2). For complexes **1b/1c** the chains are linked additionally *via* face-to-face π–π interactions [22] of the phenol rings (Table 3, Fig. S3 and S4, see ESI ‡) preventing the hydrogen atoms of the phenolic hydroxo groups from forming hydrogen bonds.

In a previous investigation it was shown that an unblocked OH group of this ligand prefers to engage in hydrogen bonding to a carbonyl group of a neighbouring metal complex.[3] This conclusion is now corroborated by the crystal structure determinations of **2a** and **2c** exhibiting the expected double hydrogen bond motif of the A ··· DD type [20] (Fig. 4, Scheme 4). In all cases **2a**–**2c** a $R^2_2(20)$ ring motif (Fig. 4, Scheme 4, Table 3) from the phenolic OH group of the ligand to the CO group (C15–O15) *trans* to the pyridine of the second complex is observed leading to a dimeric aggregate of $\bar{1}$ symmetry. The strong hydrogen bond is assisted by a weaker hydrogen bond C3–H3 ··· O15 [ring motif $R^2_2(16)$]. The ring motif found for **2a**–**2c** is topologically similar to the ring motif $R^2_2(8)$ formed by carboxylic acid dimers (Scheme 4, bottom).

The different hydrogen bonding pattern of **1a** as compared to that of **1b/1c** is also reflected in the IR spectra of the tetracarbonyl complexes in the solid state (Fig. 5). First the IR spectrum of **1a** shows a different pattern for the CO stretching vibrations due to hydrogen bonding to a different *cis*-$M(CO)_2$ moiety (equatorial/axial for **1a** and equatorial/equatorial for **1b/1c**). Second, the broad absorption for the OH stretching vibration occurs at lower energy for **1a** because of the OH ··· OH

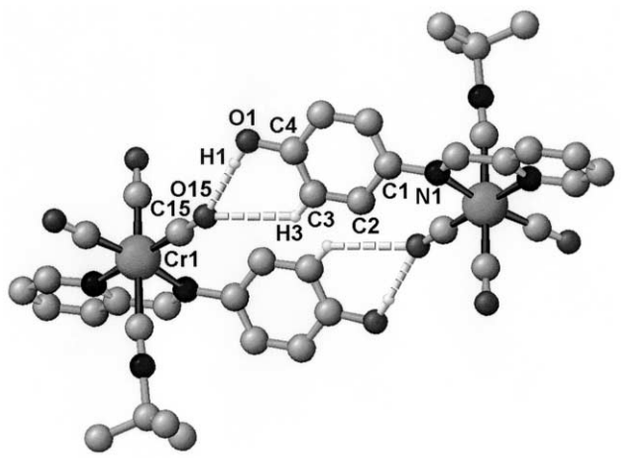

Fig. 4 Molecular structure of **2a** (and **2b/2c**) in the solid state with the $R^2_2(20)$ and $R^2_2(16)$ motifs.

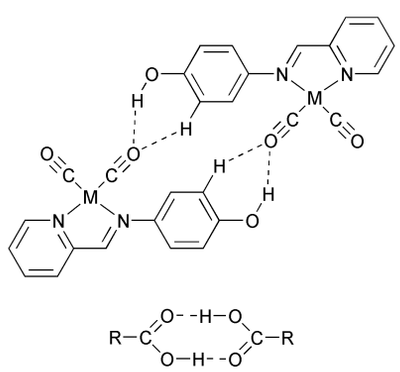

Scheme 4 Aggregation of complexes **2** in the solid state with the $R^2_2(20)$ and $R^2_2(16)$ motifs (top) and the $R^2_2(8)$ motif of the carboxylic acid dimer (bottom). M = Cr, Mo, W. Axial carbonyl and isonitrile ligands are omitted.

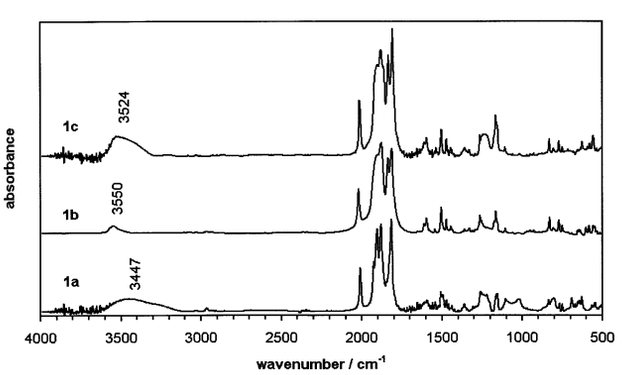

Fig. 5 IR spectra of complexes **1a**–**1c** in the solid state.

hydrogen bonding which is absent in the crystals of **1b/1c**. The latter therefore show absorptions for the OH stretching vibration at wavenumbers above 3500 cm^{-1}.

For the tricarbonyl complexes **2** a sharp and intense absorption for the OH stretching vibration is observed in the solid state at wavelengths in the range 3413–3443 cm^{-1} (Fig. 6) which

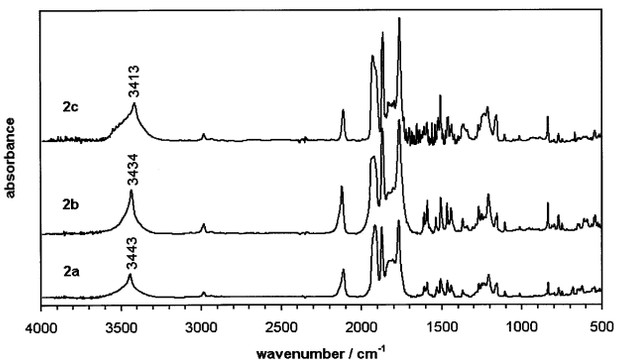

Fig. 6 IR spectra of complexes **2a**–**2c** in the solid state.

is indicative of the A ··· DD type hydrogen bond motif (Scheme 4).[3] In addition the similar pattern of the $\tilde{\nu}_{CO}$ and $\tilde{\nu}_{CN}$ absorptions substantiates the identical pattern of hydrogen bonding involving the CO group in the solid state structures of complexes **2a**–**2c**.

The O–H ··· OC hydrogen bonding in crystals of complexes **2a**–**2c** (Scheme 4) is also apparent when comparing the solution IR spectra (Fig. S2, see ESI ‡) with the solid state IR spectra (Fig. 6). The most striking difference is observed for the energy of the asymmetric vibration of the equatorial *cis*-$M(CO)_2$ fragment: in the solid state the absorption band is shifted to lower energy by 50, 41 and 57 cm^{-1} for **2a**–**2c**, respectively. DFT calculations for the model complexes $HOLMo(CO)_3CNMe$ and $HOLMo(CO)_3CNMe{\cdot}H_2O$ (Fig. S5, Tables S6–S9, see ESI ‡) with a water molecule hydrogen bonded to the corresponding carbonyl group indicate a similar red shift for this vibration (31 cm^{-1}). This shift in energy is reflected in an elongated C–O bond length found in $HOLMo(CO)_3CNMe{\cdot}H_2O$ as compared to that calculated for $HOLMo(CO)_3CNMe$ (Tables S10 and S11, see ESI ‡). The calculated $O_{carbonyl}$ ··· O_{water} distance amounts to 2.88 Å and the O_{water}–H_{water} ··· $O_{carbonyl}$ angle to 162° in reasonable agreement with the experimental values (Table 3). Although DFT calculations cannot be expected to be accurate on the level of theory used for this rather large molecule[23] the results clearly demonstrate that hydrogen bonding is responsible for the energy shifts of the CO vibrational bands.

Conclusion

Two patterns of hydrogen bonding in crystals of complexes **1** and **2** have been observed: the triple hydrogen bond of the AA ··· DDD type and the double hydrogen bond of the A ··· DD type. The former is observed whenever the OH group the Schiff base ligand is blocked while the latter is preferred if the OH group is available for hydrogen bonding to a carbonyl group. This general rule applies to all complexes of the type $[HO\text{-}(N\cap N')]M(CO)_3L$ (M = Cr, Mo, W; L = CO, CNR, THF, PPh_3) investigated so far. Even the unexpected hexamer formation of complex **1a** is in agreement with this observation. IR spectroscopy combined with theoretical calculations provides an additional means of detecting and probing hydrogen bonding patterns in crystals of complexes **1** and **2**. In the latter cases the hydrogen bonding can be inspected by IR spectroscopy from the two sides involved: the hydrogen donor unit (OH) as well as the hydrogen acceptor unit (CO).

Experimental

Unless noted otherwise, all manipulations were carried out under argon by means of standard Schlenk techniques. All solvents were dried by standard methods and distilled under argon prior to use. All other reagents were used as received from commercial sources.

NMR: Bruker Avance DPX 200 at 200.15 MHz (^1H), 50.323 MHz (^{13}C) at 303 K; chemical shifts (δ) in ppm with respect to residual solvent peaks as internal standards: CD_2Cl_2 (^1H: δ = 5.32; ^{13}C: δ = 53.8). IR spectra were recorded on a BioRad Excalibur FTS 3000 spectrometer using CaF_2 cells or CsI disks. UV/Vis/NIR spectra were recorded on a Perkin Elmer Lambda 19, 0.2 cm cells (Hellma, suprasil). Cyclic voltammetry was performed using a glassy carbon electrode, a platinum electrode and a SCE electrode, 10^{-3} M in 0.1 M nBu_4NPF_6–CH_2Cl_2, potentials are given relative to that of SCE. Mass spectra were recorded on a Finnigan MAT 8400 spectrometer, 4-nitrobenzyl alcohol (FAB). Elemental analyses were performed by the microanalytical laboratory of the Organic Chemistry Department, University of Heidelberg.

Computational method

Density functional calculations were carried out with the Gaussian98/DFT[24] series of programs. The B3LYP formulation of density functional theory was used employing the LanL2DZ basis set.[24] Harmonic vibrational frequencies and infrared intensities were calculated by numerical second derivatives using analytically calculated first derivatives.

Crystallographic structure determinations

The measurements were carried out on an Enraf-Nonius Kappa CCD diffractometer using graphite monochromated Mo-K_α radiation. The data were processed using the standard Nonius software.[25] All calculations were performed using the SHELXT PLUS software package. Structures were solved using direct or Patterson methods with the SHELXS-97 program and refined with the SHELXL-97 program.[26] Graphical handling of the structural data during refinement was performed using XMPA[27] and WinRay.[28] Atomic coordinates and anisotropic thermal parameters of the non-hydrogen atoms were refined by full-matrix least-squares calculations. Data relating to the structure determinations are collected in Tables 5 and 6.

CCDC reference numbers 168307 (**1b**), 168311 (**2b**) and 179589–179592.

See http://www.rsc.org/suppdata/dt/b2/b201647h/ for crystallographic data in CIF or other electronic format.

The syntheses of $HO\text{-}(N\cap N')$, **1b** and **2b** have been described previously.[2]

Synthesis of 1a and 1c

To a solution of $(CH_3CN)_2M(CO)_4$ (M = Cr, W[29]) (1 mmol) in 20 ml THF was added $HO\text{-}(N\cap N')$ (1 mmol) as a solid. The violet solution was evaporated to dryness and the residue was filtered through a pad of kieselgur (THF). The volume of the solution was reduced and the solution was layered with PE40/60. The resulting microcrystalline violet powder collected by filtration and dried *in vacuo*. Yields: 86% (**1a**), 90% (**1c**). Recrystallisation from acetone and PE40/60 (**1a**) and CH_2Cl_2 and PE40/60 (**1b** and **1c**) gave dark crystals suitable for X-ray crystallography.

1a. Elemental analysis. Found: C, 52.76; H, 3.45; N, 7.91. $C_{16}H_{10}N_2O_5Cr$ requires C, 53.05; H, 2.78; N, 7.73%; *m/z* (FAB) 362 (M^+, 100), 334 (M^+ − CO, 44); λ_{max}(THF) = 571 nm (3130 M^{-1} cm^{-1}); δ_H (d_6-acetone) 7.03 (br, s, 2H, *o*-C*H*), 7.51 (br, s, 2H, *m*-C*H*), 7.66 (br, s, 1H, py-*H*^{2}), 8.15 (br, s, 2H, py-*H*^{3}, py-*H*^{4}), 8.77 (br, s, 1 H, N=C*H*), 9.25 (br, s, 1H, py-*H*^{1}); δ_C(d_6-acetone) 115.9 (s, *o*-*C*H), 123.7 (s, *m*-*C*H), 126.6 (s,

Table 5 X-Ray crystallographic data for **1a**, **1b** and **1c**

	1a	**1b**	**1c**
Formula	$C_{16}H_{10}N_2O_5Cr$	$C_{16}H_{10}N_2O_5Mo$	$C_{16}H_{10}N_2O_5W$
M	362.3	406.21	494.1
Crystal dimension/mm	0.25 × 0.05 × 0.03	0.10 × 0.08 × 0.03	0.22 × 0.15 × 0.02
Crystal system	Trigonal	Monoclinic	Monoclinic
Space group (no.)	$R\bar{3}$ (148)	$P2_1/c$ (14)	$P2_1/c$ (14)
a/Å	35.203(5)	9.056(2)	9.004(2)
b/Å	35.203(5)	24.644(5)	24.712(5)
c/Å	6.526(1)	7.091(1)	7.073(1)
α/°	90.0(0)	90.0(0)	90.0(0)
β/°	90.0(0)	108.93(3)	108.99(3)
γ/°	120.0(0)	90.0(0)	90.0(0)
Cell volume/Å^3	7004(2)	1497.0(5)	1488.1(5)
Molecular units per cell	18	4	4
μ/mm^{-1}	0.764	0.906	7.793
Density (calc)/g cm^{-3}	1.546	1.802	2.205
T/K	200	200	200
Scan range (2θ)	4.0–55.0	4.8–60.1	3.3–60.1
Scan speed/sec frame^{-1}	80	10	20
Measured reflections	46190	3781	8040
Unique reflections	3566	2765	4338
Obs. reflections ($I \geq 2\sigma$)	2471	1860	3002
Parameters refined	220	226	222
Max. of residual electron density/e Å^{-3}	0.78/−0.41	1.55/−0.59	3.50/−1.47
Agreement factors	$R_1 = 4.5\%$	$R_1 = 6.7\%$	$R_1 = 5.3\%$
(F^2 refinement)	$R_w = 10.7\%$	$R_w = 12.4\%$	$R_w = 13.3\%$

Table 6 X-Ray crystallographic data for **2a**, **2b** and **2c**

	2a	**2b**	**2c**
Formula	$C_{20}H_{19}N_3O_4Cr$	$C_{20}H_{19}N_3O_4Mo$	$C_{20}H_{19}N_3O_4W$
M	417.4	461.33	549.2
Crystal dimension/mm	0.50 × 0.20 × 0.05	0.40 × 0.20 × 0.03	0.40 × 0.20 × 0.03
Crystal system	Monoclinic	Monoclinic	Monoclinic
Space group (no.)	$P2_1/n$ (14)	$P2_1/n$ (14)	$P2_1/n$ (14)
a/Å	11.469(2)	11.576(2)	11.578(2)
b/Å	12.979(3)	13.114(3)	12.995(3)
c/Å	13.105(3)	13.293(3)	13.271(3)
β/°	91.81(3)	92.89(3)	92.19(3)
Cell volume/Å^3	1949.8(7)	2015.4(7)	1995.2(7)
Molecular units per cell	4	4	4
μ/mm^{-1}	0.618	0.681	5.820
Density (calc)/g cm^{-3}	1.422	1.520	1.828
T/K	200	200	200
Scan range (2θ)	4.4–60.1	4.4–60.0	4.4–60.0
Scan speed/sec frame^{-1}	15	5	20
Measured reflections	10810	10509	10638
Unique reflections	5681	5858	5837
Obs. reflections ($I \geq 2\sigma$)	4157	4072	3822
Parameters refined	329	329	259
Max. of residual electron density/e Å^{-3}	0.32/−0.47	0.76/−0.55	5.33/−2.41
Agreement factors	$R_1 = 4.1\%$	$R_1 = 4.2\%$	$R_1 = 7.7\%$
(F^2 refinement)	$R_w = 10.9\%$	$R_w = 8.4\%$	$R_w = 18.7\%$

py-C^2), 128.7 (s, py-C^4), 137.6 (s, py-C^3), 146.6 (s, *p*-*C*), 153.5 (s, py-C^1), 155.9 (s, *i*-*C*), 158.0 (s, py-C^5), 162.8 (s, N=*C*H), 213.1, 227.9, 230.9 (s, *C*O); IR (THF) 2006 (m, CO), 1899 (vs, CO), 1846 (s, CO); IR (CsI) 3447 (br, OH), 2008 (m, CO), 1925 (vs, CO), 1903 (vs, CO), 1880 (vs, CO), 1815 (s, CO); CV (CH_2Cl_2) $E_{1/2}$ 425 mV (rev.).

1c. Elemental analysis. Found: C, 39.15; H, 2.30; N, 5.64. $C_{16}H_{10}N_2O_5W$ requires C, 38.89; H, 2.04; N, 5.67%; *m*/*z* (FAB) 494 (M^+, 100), 466 ($M^+ - CO$, 83); λ_{max}(THF) = 553 nm (9010 $M^{-1}cm^{-1}$); δ_H (d_6-acetone) 7.02 (d, 2H, *o*-C*H*, $^3J_{HH}$ = 8.8 Hz), 7.61 (d, 2H, *m*-C*H*, $^3J_{HH}$ = 8.8 Hz), 7.68–7.74 (m, 1H, py-H^2), 8.23 (dvt, 1H, py-H^4, J_{HH} = 1.4/7.5 Hz), 8.32 (d, 1H, py-H^3, J_{HH} = 7.2 Hz), 9.22 (s, 1 H, N = C*H*), 9.31 (d, 1H, py-H^1, $^3J_{HH}$ = 5.1 Hz); δ_C(d_6-acetone) 115.9 (s, *o*-*C*H), 124.5 (s, *m*-*C*H), 127.9 (s, py-C^2), 129.7 (s, py-C^4), 138.3 (s, py-C^3), 145.3 (s, *p*-*C*), 153.1 (s, py-C^1), 156.7 (s, *i*-*C*), 158.5 (s, py-C^5), 164.4 (s, N=*C*H), 199.6, 214.2, 217.1 (s, *C*O); IR (THF) 2005 (m, CO), 1892 (vs, CO), 1846 (s, CO); IR (CsI) 3524 (br, OH), 2010 (m, CO), 1902 (vs, CO), 1879 (vs, CO), 1833 (s, CO), 1808 (s, CO); CV (CH_2Cl_2) E_p 720 mV (irr.).

Synthesis of 2a and 2c

To a solution of $(CH_3CN)_3M(CO)_3$ (M = Cr, W[29]) (1 mmol) in 20 ml THF was added HO-(N∩N′) (1 mmol) as a solid. To the blue solution was added 0.11 ml (1 mmol) CN*t*Bu. The green solution was evaporated to dryness and the residue was filtered through a pad of kieselgur (THF). The volume of the solution was reduced and the solution was layered with PE40/60. The resulting microcrystalline powder was collected by filtration and dried *in vacuo*. Yields: 95% (**2a**), 62% (**2b**). Recrystallisation from CH_2Cl_2 and PE40/60 (**2a**–**2c**) gave dark crystals suitable for X-ray crystallography.

2a. Elemental analysis. Found: C, 56.71; H, 4.59; N, 10.13. $C_{20}H_{19}N_3O_4Cr$ requires C, 57.55; H, 4.59; N, 10.07%; *m*/*z* (FAB)

417 (M^+, 14), 333 (M^+–3CO, 100); λ_{max}(THF) = 665 nm (5450 M^{-1} cm^{-1}); δ_H (d_6-acetone) 1.21 (s, 9H, CH_3), 6.90 (br, s, 2H, *o*-C*H*), 7.3–7.4 (m, 3H, *m*-C*H* + py-H^2), 7.87 (br, s, 2H, py-H^3, py-H^4), 8.62 (br, s, 1 H, N=C*H*), 9.22 (br, s, 1H, py-H^1); δ_C(d_6-acetone) 30.6 (s, *C*H_3), 115.6 (s, *o*-*C*H), 123.7 (s, *m*-*C*H), 125.0 (s, py-C^2), 127.9 (s, py-C^4), 135.7 (s, py-C^3), 147.1 (s, *p*-*C*), 152.6 (s, py-C^1), 156.3 (s, *i*-*C*), 157.6 (s, py-C^5), 160.0 (s, N=*C*H), 169.2 (s, *C*N), 218.3, 233.6, 237.7 (s, *C*O); IR (THF) 2110 (m, CN), 1917 (vs, CO), 1846 (s, CO), 1818 (s, CO); IR (CsI) 3443 (m, OH), 2113 (m, CN), 1914 (vs, CO), 1871 (s, CO), 1768 (s, CO); CV (CH_2Cl_2) $E_{1/2}$ 25 mV (qrev.; reverse scan: −230 mV).

2c. Elemental analysis. Found: C, 43.48; H, 3.67; N, 7.47. $C_{20}H_{19}N_3O_4W$ requires C, 43.74; H, 3.49; N, 7.65%; *m*/*z* (FAB) 549 (M^+, 56), 521 (M^+ − CO, 100); λ_{max}(THF) = 630 nm (10810 M^{-1} cm^{-1}); δ_H (d_6-acetone) 1.21 (s, 9H, *C*H_3), 6.89 (d, 2H, *o*-C*H*, $^3J_{HH}$ = 8.5 Hz), 7.53 (d, 2H, *m*-C*H*, $^3J_{HH}$ = 8.5 Hz), 7.4–7.5 (m, 1H, py-H^2), 7.96 (dvt, 1H, py-H^4, J_{HH} = 1.4/7.5 Hz), 8.09 (d, 1H, py-H^3, J_{HH} = 7.8 Hz), 9.07 (s, 1 H, N=C*H*), 9.19 (d, 1H, py-H^1, $^3J_{HH}$ = 5.5 Hz); δ_C(d_6-acetone) 30.5 (s, *C*H_3), 115.7 (s, *o*-*C*H), 124.6 (s, *m*-*C*H), 126.7 (s, py-C^2), 128.9 (s, py-C^4), 136.3 (s, py-C^3), 146.1 (s, *p*-*C*), 151.9 (s, py-C^1), 157.2 (s, *i*-*C*), 158.1 (s, py-C^5), 161.6 (s, N=*C*H), 204.1, 220.6, 224.6 (s, *C*O), *C*N n.o.; IR (THF) 2106 (m, CN), 1915 (vs, CO), 1842 (s, CO), 1817 (s, CO); IR (CsI) 3413 (m, OH), 2112 (m, CN), 1926 (vs, CO), 1863 (s, CO), 1760 (s, CO); CV (CH_2Cl_2) E_p 730 mV (irr.).

Acknowledgements

This work was supported by the Deutsche Forschungsgemeinschaft and the Fonds der Chemischen Industrie. The permanent, generous support from Prof. Dr. G. Huttner is gratefully acknowledged. We thank Yasmin Nisar for preparative assistance.

References and notes

1 K. Heinze, U. Winterhalter and T. Jannack, *Chem. Eur. J.*, 2000, **6**, 4203–4210.
2 K. Heinze, *Chem. Eur. J.*, 2001, **7**, 2922–2932.
3 K. Heinze, *J. Chem. Soc., Dalton Trans.*, 2002, 540–547.
4 D. Braga, F. Grepioni, K. Biradha, V. R. Pedireddi and G. R. Desiraju, *J. Am. Chem. Soc.*, 1995, **117**, 3156–3166.
5 T. Steiner, *Angew. Chem.*, 2002, **114**, 50–80; T. Steiner, *Angew. Chem., Int. Ed.*, 2002, **41**, 48–76.
6 D. Braga, *J. Chem. Soc., Dalton Trans.*, 2000, 3705–3713.
7 H. Behrens, E. Lindner and G. Lehnert, *J. Organomet. Chem.*, 1970, **22**, 439–448.
8 B. Bildstein, M. Malaun, H. Kopacka, M. Fontani and P. Zanello, *Inorg. Chim. Acta*, 2000, **300–302**, 16–22.
9 M. N. Ackermann, W. G. Fairbrother, N. S. Amin, C. J. Deodene, C. M. Lamborg and P. T. Martin, *J. Organomet. Chem.*, 1996, **523**, 145–151.
10 E. C. Alyea and V. K. Jain, *Polyhedron*, 1995, **15**, 1723–1730.
11 $R^x_y(n)$: The superscript *x* denotes the number of hydrogen acceptors, the subscript *y* the number of hydrogen donors and *n* the ring size. C(*n*) denotes a chain with *n* atoms in the repeating unit. J. Bernstein, R. E. Davis, L. Shimoni and N.-L. Chang, *Angew. Chem.*, 1995, **107**, 1689–1708; J. Bernstein, R. E. Davis, L. Shimoni and N.-L. Chang, *Angew. Chem., Int. Ed. Engl.*, 1995, **34**, 1555–1574.
12 G. Ferguson, C. D. Carroll, C. Glidewell, C. M. Zakaria and A. J. Lough, *Acta Crystallogr. Sect. B*, 1995, **51**, 367–377.
13 R. J. Doedens, E. Yohannes and M. Ishaque Khan, *Chem. Commun.*, 2002, 62–63.
14 M. Razavet, A. Le Cloirec, S. C. Davies, D. L. Hughes and C. J. Pickett, *J. Chem. Soc., Dalton Trans.*, 2001, 3551–3552.
15 R. Custelcean, C. Afloroaei, M. Vlassa and M. Polverejan, *Angew. Chem.*, 2000, **112**, 3224–3226; R. Custelcean, C. Afloroaei, M. Vlassa and M. Polverejan, *Angew. Chem., Int. Ed.*, 2000, **39**, 3094–3096.
16 R. Ludwig, *ChemPhysChem*, 2000, **1**, 53–56.
17 K. Nauta and R. E. Miller, *Science*, 2000, **287**, 293–295.
18 S. S. Xantheas and T. H. Dunning Jr., *J. Chem. Phys.*, 1993, **99**, 8774–8792.
19 S. S. Xantheas, *J. Chem. Phys.*, 1995, **102**, 4505–4517.
20 This nomenclature summarises the sequence of hydrogen bond donor (D) and acceptor groups (A) on each of the interacting molecules.
21 $R^6_6(36)$ compares to C(6), $R^6_6(42)$ to C(7) and $R^6_6(48)$ to C(8).
22 C. Janiak, *J. Chem. Soc., Dalton Trans.*, 2000, 3885–3896.
23 W. Koch and M. C. Holthausen, *A Chemist's Guide to Density Functional Theory*, Wiley-VCH, Weinheim, 2001.
24 M. J. Frisch, G. W. Trucks, H. B. Schlegel, G. E. Scuseria, M. A. Robb, J. R. Cheeseman, V. G. Zakrzewski, J. A. Montgomery, Jr., R. E. Stratmann, J. C. Burant, S. Dapprich, J. M. Millam, A. D. Daniels, K. N. Kudin, M. C. Strain, O. Farkas, J. Tomasi, V. Barone, M. Cossi, R. Cammi, B. Mennucci, C. Pomelli, C. Adamo, S. Clifford, J. Ochterski, G. A. Petersson, P. Y. Ayala, Q. Cui, K. Morokuma, D. K. Malick, A. D. Rabuck, K. Raghavachari, J. B. Foresman, J. Cioslowski, J. V. Ortiz, B. B. Stefanov, G. Liu, A. Liashenko, P. Piskorz, I. Komaromi, R. Gomperts, R. L. Martin, D. J. Fox, T. Keith, M. A. Al-Laham, C. Y. Peng, A. Nanayakkara, C. Gonzalez, M. Challacombe, P. M. W. Gill, B. Johnson, W. Chen, M. W. Wong, J. L. Andres, C. Gonzalez, M. Head-Gordon, E. S. Replogle and J. A. Pople, Gaussian 98, revision A.6, Gaussian, Inc., Pittsburgh, PA, 1998, http://www.gaussian.com.
25 R. Hooft, Collect, Data Collection Software, Nonius, The Netherlands, 1998, http://www.nonius.com.
26 G. M. Sheldrick, SHELXS-97, Program for Crystal Structure Solution, University of Göttingen, Germany, 1997, http://shelx.uni-ac.gwdg.de/shelx/. G. M. Sheldrick, SHELXL-97, Program for Crystal Structure Refinement, University of Göttingen, Germany, 1997, http://shelx.uni-ac.gwdg.de/shelx/; *International Tables for X-ray Crystallography*, Kynoch Press, Birmingham, UK, 1974, vol. 4.
27 L. Zsolnai and G. Huttner, *XPMA*, University of Heidelberg, Germany, 1998, http://www.rzuser.uni-heidelberg.de/~il1/laszlo/xpm.html.
28 R. Soltek and G. Huttner, *WinRay*, University of Heidelberg, Germany, 1999, http://www.uni-heidelberg.de/institute/fak12/AC/huttner/html/winray.html.
29 G. R. Dobson, M. F. Amr El Sayed, I. W. Stolz and R. K. Shelline, *Inorg. Chem.*, 1962, **1**, 526–530.